PROCEEDINGS OF SCIENCE

Highlights from muon $g-2$

Saskia Charity[a,*]

[a] *University of Liverpool,United Kingdom*

[b] *On behalf of the Fermilab Muon g − 2 Collaboration*

E-mail: s.charity@liverpool.ac.uk

In June 2025, the Fermilab Muon $g-2$ Experiment announced its final measurement of the muon anomalous magnetic moment a_μ, to a precision of 127 parts per billion [1]. This result was the culmination of six years of data-taking. The measurement is consistent with the current Standard Model (SM) value, provided by the $g-2$ Theory Initiative's latest White Paper [2], which uses lattice QCD techniques to compute the non-perturbative hadronic terms. This contribution will cover the details presented in the publication and discuss the implications of the result in the context of the theoretical (SM) landscape.

The European Physical Society Conference on High Energy Physics (EPS-HEP2025)
7-11 July 2025
Marseille, France

*Speaker

 ISSN 1824-8039 . Published by SISSA Medialab.

PoS(EPS-HEP2025)037

1. Introduction

The Fermilab Muon $g-2$ Experiment recorded data between 2018 and 2023. The first dataset (Run−1), was recorded in 2018 and published in 2021 [3]. The second publication in 2023, [4], reflects runs 2 and 3 collected between 2019 and 2020. The analysis techniques are fully documented in [5]. The recent publication, which this conference talk discusses, contains the result of data analysis on runs 4-6, collected between 2021 and 2023. The statistics for each dataset are shown in figure 1.

The results presented in this contribution are published in [1]. The data-taking techniques will be described and the analysis strategy for the final result will be presented. Details of the experimental design and analysis techniques are fully covered in the Fermilab $g-2$ Collaboration's previous publications [1, 3, 4, 6–8]. Relevant details will be explored in more details in this contribution, in particular the discussion of dedicated measurements and analysis improvements involved in the publication of the full dataset.

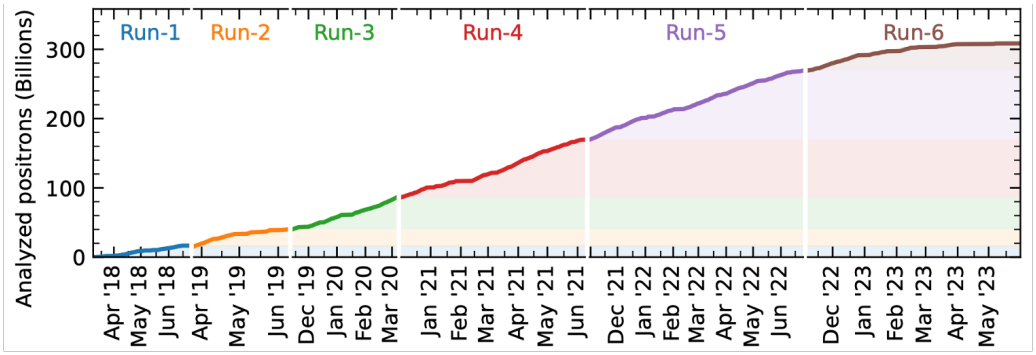

Figure 1: The amount of data collected during each run period of the $g-2$ Experiment.

2. The Fermilab Muon $g-2$ Experiment

The Fermilab experiment uses a beam of 3.1 GeV/c polarized muons produced at the Fermilab muon campus. The muons are injected into a magnetic storage ring with a diameter of 14 m and a homogeneous vertical magnetic field of strength 1.45 T in the muon storage region. The magnetic field provides weak radial focusing and defines the axis of muon spin precession. The magnet is the same as was used in the Brookhaven experiment [9], and was moved to Fermilab in 2013. The vertical magnetic field focuses the beam radially and enables the muons to be stored in the ring, circulating around the azimuth of the ring until they decay to positrons. Having a lower momentum than their parent muons, the positrons follow a tighter radial path and so they spiral into the centre of the ring, where they are intercepted by a suite of 24 PbF_2 electromagnetic calorimeters. A brief description of the key stages of the experiment follows.

1. **Injection** The polarized muons are injected into the magnetic storage ring through an inflector magnet which shields the muons from the storage ring magnetic field during their injection.

2. **Fast muon kicker** Muons from the inflector are injected at a slightly higher angle than the ideal orbit at the centre of the storage ring radius. To keep the muons in the storage ring, a fast

radial magnetic 'kick' is applied to the muons to move them onto the correct trajectory. The kicker magnets apply a vertical magnetic field in the opposite direction of the main storage field and pushes the muon beam inwards. The kicker pulse must be synchronised with the muon injection time. The fast kicker field must be delivered during the first orbit of the beam only, since any residual pulsing will result in applying an unnecessary extra kick to the muons that are already on the right path. Residual charge in the kicker system results in a small transient field that slightly perturbs the muon beam after the first turn, contributing a correction term and associated systematic uncertainty that must be measured directly. This is discussed later on. For more details on the kicker system see ref. [10].

3. **Vertical focusing with electrostatic quadrupoles** The magnetic storage ring provides radial focusing only. Vertical focusing is provided by a suite of electrostatic quadrupoles (ESQs) which cover 43% of the azimuth of the ring. A second transient magnetic field is associated with the vibration of the ESQ plates during pulsing which leads to an additional transient magnetic field, experienced by the muons during storage but which cannot be measured by the NMR probes inside the ring.

4. **Muon spin precession** The muons circulate inside the storage ring with cyclotron frequency ω_c. While they orbit, their spins precess about the vertical magnetic field with spin precession frequency ω_s. The parity-violating nature of Weak decays means that the spin of the parent muon is encoded in that of the daughter electron, with the highest-energy electrons being emitted in the direction of the muon spin. This results in the oscillation of the number of electrons detected above an energy threshold oscillating at the anomalous spin precession frequency, ω_a, given by:
$$\omega_a = \omega_s - \omega_c. \tag{1}$$

5. **Magnetic field measurement** The experiment measures the ratio of two frequencies:
$$R'_\mu = \frac{\omega_a}{\tilde{\omega'_p}(T_r)} \tag{2}$$
where $\tilde{\omega'_p}(T_r)$ is the nuclear magnetic resonance (NMR) precession frequency of shielded protons in a spherical water sample corrected to a reference temperature T_r, averaged over the muon beam distribution, and ω_a is as defined in equation 1. A map of the magnetic field contours inside the muon storage ring is shown in figure 3, overlaid with the stored muon beam profile measured by tracking detectors located at 180° and 270° from the inflector exit. The uncertainty budget of the experiment requires equal uncertainties from the ω_a and $\tilde{\omega'_p}(T_r)$ terms, and the measurement strategy for the magnetic field term is discussed in more detail later.

3. Measuring the muon anomalous magnetic moment a_μ

The muon anomalous magnetic moment a_μ is extracted from the ratio of the two frequencies ω_a and $\tilde{\omega'_p}(T_r)$, and some well-known external constants:
$$a_\mu = \frac{\omega_a}{\tilde{\omega'_p}(T_r)} \frac{\mu'_p}{\mu_B} \frac{m_\mu}{m_e} \tag{3}$$

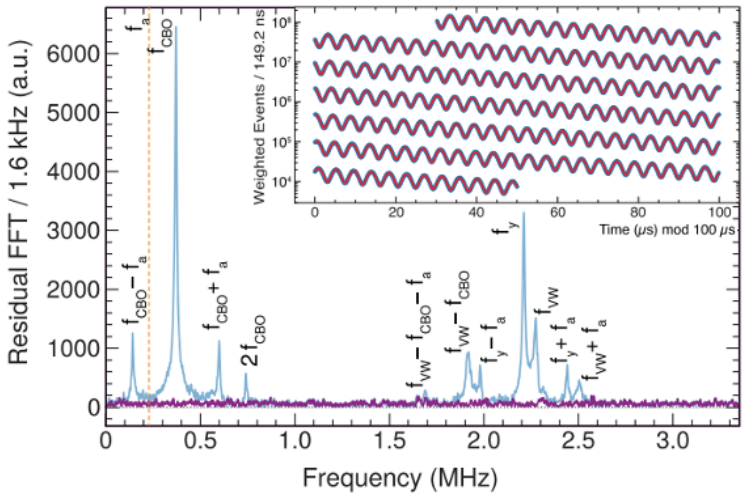

Figure 2: The fitted spin precession oscillation. Figure taken from [1].

where $\frac{\mu'_p}{\mu_B}$ and $\frac{m_\mu}{m_e}$ are taken from CODATA [11] and have uncertainties of 4 ppb and 22 ppb respectively.

4. Measuring the anomalous precession frequency ω_a

The anomalous precession frequency ω_a is determined from the oscillation in the number of detected positrons above an energy threshold. An example of this oscillation is shown in figure 2. A total of 8 different analysis methods are used by 5 different analysis groups, resulting in a total of 20 different analyses. At first order, the frequency ω_a can be extracted from a simple five-parameter fit that includes the sinusoidal oscillation and decaying exponential terms. To achieve the required precision however, over 30 fit parameters are required to account for additional oscillations present in the spectrum, including additional frequencies associated with the motion of the muon beam inside the storage ring. The Fast Fourier Transform (FFT) of the residuals of the five-parameter fit to the ω_a data is shown in figure 2. Large peaks indicate the presence of additional oscillations that are not accounted for by the simple fit. Care must be taken to set the operating conditions of the experiment such that none of these frequencies are close to ω_a. Each frequency in the fit must be determined independently and each has an associated uncertainty. After accounting for all of the additional terms in the fit, the extracted frequency ω_a is modified by $O(1\text{ppm})$. For further details about the analysis strategy, see [5, 7].

5. Measuring the muon-weighted magnetic field $\tilde{\omega'_p}(T_r)$

There are several steps to measuring the magnetic field term.

1. **Mapping the magnetic field with the in-vacuum NMR trolley** The magnetic field map in the muon storage region must be measured periodically using an in-vacuum 'trolley' containing an array of 17 pulsed NMR probes. Every 3-4 days, the muon beam is stopped for $\sim$ 4 hours and the trolley is inserted into the storage ring. The trolley is driven around

the full azimuth of the ring and maps out the magnetic field contours in the storage region at approximately 9000 different azimuthal positions. For further details about the trolley measurements and the NMR techniques used see [6, 12].

2. **Tracking field changes with 'fixed' NMR probes** 372 NMR probes, the same design as those in the trolley, are embedded in the muon storage ring vacuum chambers, located above and below the muon storage region. These track changes in the muon field components over time during the muon storage, since the trolley cannot be present during muon beam data-taking.

3. **Field interpolation** The measurements of the fixed probes must be calibrated using the measurements of the trolley data, which is more accurate and has more degrees of freedom (is sensitive to higher-order field gradients) than the fixed probes. When the trolley drives past a fixed probe station the differences between the trolley and fixed probe measurements are calculated and used to correct the fixed probe measurements. These differences change over time, and so the trolley corrections at a given time between the two measurements is calculated as the weighted average of the corrections in the two trolley runs. The analysis techniques are fully documented in [5, 6].

4. **Absolute calibration** The cylindrical NMR probes in the trolley and the fixed probes use a petroleum NMR medium. In order to express a_μ in the form given in equation 3, the measured field must be calibrated to give the Larmor frequency of protons in a spherical water sample at a reference temperature of $25°C$. A dedicated campaign of measurements enables this calibration. During beam-off periods, a cylindrical probe containing H_2O is inserted into a region of the magnet where it measures the same field as the trolley, and this is repeated a number of times. The cylindrical probe is calibrated against other well-known probes in a separate campaign of measurements in an MRI magnet at Argonne National Laboratory (ANL). For further details about the calibration campaign, see [6, 13].

6. Corrections and Uncertainties

The full expression for the ratio of ω_a and $\tilde{\omega_p'}(T_r)$ is given by:

$$a_\mu = \frac{f_{clock}\,\omega_a(1 + C_E + C_p + C_{pa} + C_{dd} + C_{ml})}{f_{calib}\langle\omega_p'(T_r) \times M\rangle(1 + B_k + B_q)} \tag{4}$$

where

- f_{calib} is the clock blinding frequency. As in previous runs, the clock frequency is blinded in such a way that the true frequency is not known to analyzers. This frequency is only subtracted from the measured value of ω_a at the final stage of the analysis after a unanimous vote from the collaboration.

- C_E, C_p, C_{pa}, C_{dd} and C_{ml} are corrections related to the dynamics of the muon beam. C_E is the largest correction, with a value of 347 ppb and an uncertainty of 27 ppb, and is associated with the momentum spread of the muon beam.

- B_k and B_q are the fast transient magnetic fields from the kicker and quadrupole systems, discussed earlier, and

- M is the measured muon beam distribution.

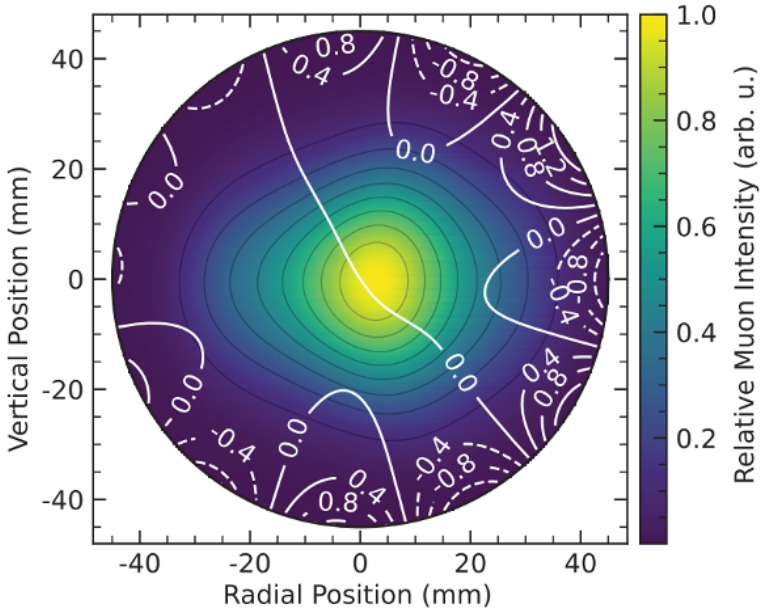

Figure 3: The beam profile in runs 4-6 of the experiment overlaid with the azimuthally-averaged magnetic field contours. Figure taken from [1].

7. Systematic uncertainties

The systematic uncertainty table is given in table I of [1]. The total uncertainty on a_μ is 139 ppb, of which 114 ppb is statistical uncertainty from the anomalous spin precession analysis, and 76 ppb is systematic. The different uncertainties range from 2 to 34 ppb. There is no clear dominant source of systematic, as several different uncertainties have similar values. Reducing the overall systematic uncertainty on a_μ would require a reduction in many different categories.

Many of the systematic uncertainties were already at their design target in the Run-2/3 dataset. However, for the final dataset, several corrections and uncertainties were cross-checked to ensure they were determined accurately. The kicker transient magnetic field correction was studied in greater detail using two measurement techniques. Time-dependent residual magnetic fields from the kicker magnets were measured during beam-off periods with two separate magnetometers. One magnetometer uses optical fibers to guide laser light into the kicker region, and the other used an open laser beam guided into the storage region through a window and using mirrors to guide the light. For Run-4/5/6, several transverse positions were studied.

8. Conclusion and outlook

The Fermilab muon $g-2$ experiment completed its data-taking in 2023 and published its final result of the muon anomalous magnetic moment, a_μ, in 2025 [1]. The final experimental average is shown in figure 4. Over the six years of running, a_μ was measured in 11 different datasets with different running conditions, and the results are consistent within uncertainties, as shown in figure 7. Figure 6 shows ω_a vs $\tilde{\omega}'_p(T_r)$ for the different datasets in Run-456. The consistency of the different datasets is discussed further in [14]. The Muon $g-2$ Theory Initiative published an updated Standard Model prediction earlier this year [2]. Their updated prediction includes only lattice QCD values for the non-perturbative hadronic vacuum polarization (HVP) terms, and is in agreement with the Fermilab measurement. However, the situation is complex as there exist significant tensions between lattice HVP treatments and an alternative treatment using dispersive approach to determine a_μ^{HVP} from hadronic cross-sections measured at e^+e^- colliders. The current comparison with the Standard Model is shown in figure 5, using data taken from [2].

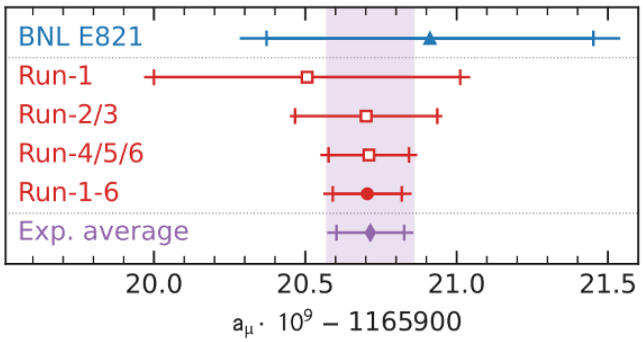

Figure 4: The experimental average of a_μ measured in the different $g-2$ publications. Taken from ref. [1].

9. Acknowledgements

I would like to acknowledge my colleagues in the Fermilab $g-2$ Collaboration for their support. This work was supported by the Science and Technology Facilities Council (STFC).

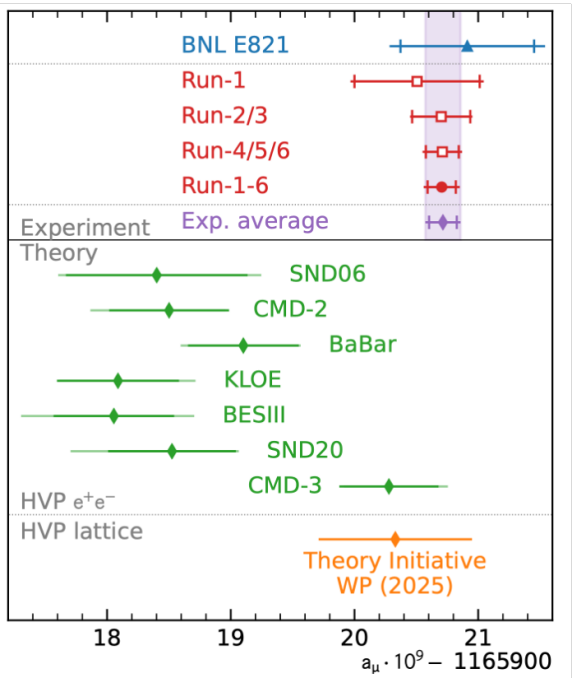

Figure 5: Top part: the experimental values of a_μ measured at the BNL and Fermilab experiments. Middle part (green points): the different values of a_μ^{SM} where the HVP terms are calculated via a dispersion relation with hadronic cross-sections measured at the listed experiments. Bottom part (orange): the value of a_μ^{SM} from [2], which uses lattice QCD approaches to evaluate a_μ^{HVP}.

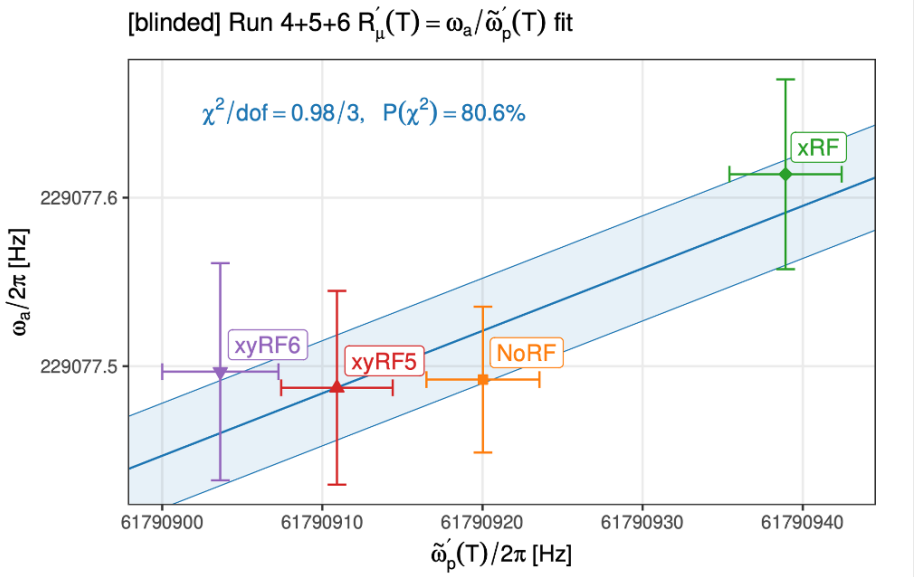

Figure 6: The measured muon-weighted magnetic field term vs the measured anomalous spin precession frequency for each dataset in the Run-4/5/6 analysis.

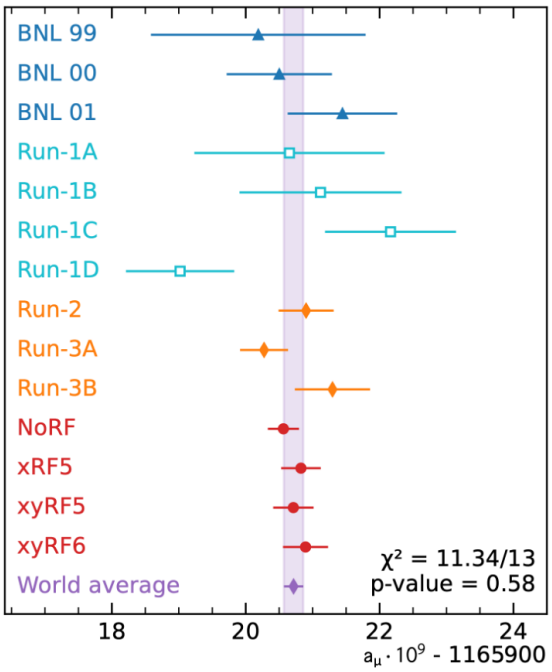

Figure 7: Measured values of a_μ for each dataset in the Fermilab and Brookhaven $g-2$ experiments.

References

[1] D. P. Aguillard et al. Measurement of the positive muon anomalous magnetic moment to 127 ppb. *Phys. Rev. Lett.*, 135(10):101802, 2025.

[2] R. Aliberti et al. The anomalous magnetic moment of the muon in the standard model: an update. *Physics Reports*, 1143:1–158, 2025.

[3] B. Abi et al. Measurement of the positive muon anomalous magnetic moment to 0.46 ppm. *Phys. Rev. Lett.*, 126:141801, Apr 2021.

[4] D. P. Aguillard et al. Measurement of the positive muon anomalous magnetic moment to 0.20 ppm. *Phys. Rev. Lett.*, 131:161802, Oct 2023.

[5] D. P. Aguillard et al. Detailed report on the measurement of the positive muon anomalous magnetic moment to 0.20 ppm. *Phys. Rev. D*, 110:032009, Aug 2024.

[6] T. Albahri et al. Magnetic-field measurement and analysis for the muon $g-2$ experiment at Fermilab. *Phys. Rev. A*, 103:042208, Apr 2021.

[7] T. Albahri et al. Measurement of the anomalous precession frequency of the muon in the Fermilab muon $g-2$ experiment. *Phys. Rev. D*, 103:072002, Apr 2021.

[8] T. Albahri et al. Beam dynamics corrections to the run-1 measurement of the muon anomalous magnetic moment at Fermilab. *Phys. Rev. Accel. Beams*, 24:044002, Apr 2021.

[9] G. W. Bennett et al. Final report of the E821 muon anomalous magnetic moment measurement at BNL. *Phys. Rev. D*, 73:072003, Apr 2006.

[10] A. P. Schreckenberger et al. The fast non-ferric kicker system for the muon g-2 experiment at Fermilab. *Nuclear Instruments and Methods A*, 1011(165597), 2021.

[11] D. B. Newell P. J. Mohr, E. Tiesinga and B. N. Taylor. Codata recommended values of the fundamental physical constants: 2022. *Review of Modern Physics*, 97(025002), 2025.

[12] S. Corrodi, P. De Lurgio, D. Flay, J. Grange, R. Hong, D. Kawall, M. Oberling, S. Ramachandran, and P. Winter. Design and performance of an in-vacuum, magnetic field mapping system for the muon g-2 experiment. *Journal of Instrumentation*, 15(11):P11008, Nov 2020.

[13] D. Flay, D. Kawall, T. Chupp, S. Corrodi, M. Farooq, M. Fertl, J. George, J. Grange, R. Hong, R. Osofsky, S. Ramachandran, E. Swanson, and P. Winter. High-accuracy absolute magnetometry with application to the Fermilab muon g-2 experiment. *Journal of Instrumentation*, 16(12):P12041, Dec 2021.

[14] Alberto Lusiani. Combination and checks of highly correlated measurements of the muon precession frequency in magnetic field for the FNAL measurement of muon $g-2$. EPS-HEP, 2025.